Impact of thickness and heat treatment on some physical properties of thin Cu$_2$SnS$_3$ films

Iqbal S. Naji, Hoolya Abdulrasool

Department of Physics, College of Science, University of Baghdad, Baghdad, Iraq

E-mail: moon_moonaaaa@yahoo.com

Abstract

Copper tin sulfide (Cu$_2$SnS$_3$) thin films have been grown on glass substrate with different thicknesses (500, 750 and 1000) nm by flash thermal evaporation method after prepare its alloy from their elements with high purity. The as-deposited films were annealed at 473 K for 1h. Compositional analysis was done using Energy dispersive spectroscopy (EDS). The microstructure of CTS powder examined by SEM and found that the large crystal grains are shown clearly in images. XRD investigation revealed that the alloy was polycrystalline nature and has cubic structure with preferred orientation along (111) plane, while as deposited films of different thickness have amorphous structure and converted to polycrystalline with annealing temperature for high thickness. AFM measurements showed that the grain size of the films was increasing by annealing. The ultraviolet- visible absorption spectrum measurement indicated that the films have a direct energy band gap. E$_g$ decrease with thickness and increase with annealing.

تأثير السمك والمعاملة الحرارية على بعض الخصائص الفيزيائية لاغشية Cu$_2$SnS$_3$ الرقيقة

اقبال سهام ناجي، هوليا عبدالرسول لفته

قسم الفيزياء، كلية العلوم، جامعة بغداد، بغداد، العراق

الخلاصـــة

تم ترسيب أغشية Cu$_2$SnS$_3$ الرقيقة على قواعد من الزجاج وبسمك مختلف (500، 750، 1000) نانومتر بطريقة التبخير الحراري الوميضي بعد تحضير السبيكة من عناصرها وبنقاوة عالية. تم معاملة الاغشية المرسبة حراريا عند 473 كلفن لمدة ساعة واحدة. تم تحليل المكونات بأستخدام مجهر تفريق الطاقة (EDS) وتم اختبار التركيب الدقيق لمسحوق CTS بأستخدام المجهر الالكتروني الماسح (SEM) وأوضحت الصور وجود حبيبات بلورية كبيرة. اظهرت قياسات حيود الاشعة السينية (XRD) ان السبيكة كانت ذات تركيب متعدد التبلور ولها تركيب مكعب باتجاه مفضل (111) بينما الاغشية المرسبة ولسمك مختلف تمتلك تركيب عشوائي ويتحول الى متعدد التبلور عند تلدينها بدرجة 473 كلفن للسمك العالي. بينت قياسات مجهر القوة الذرية (AFM) ان الحجم الحبيبي للاغشية يزداد بالتلدين. تشير قياسات طيف ألامتصاص للاشعة فوق البنفسجية ـ مرئية الى أن الاغشية تمتلك فجوة طاقة مباشرة وان E$_g$ تقل بأزدياد السمك وتزداد بالتلدين.

Introduction

The energy crisis and environment problems becoming more and more serious, it is very urgent to explore new energy resource, Solar energy is a promising new energy resource which is clean and sustainable [1]. In recent years, there has been a great deal of interest in the study of nontoxic semiconductors from both the fundamental and technological points of view for solar cell materials [2]. The I-IV-VI ternary group of semiconductor was attracted much attention because of their interesting properties [3]. The multiple local coordination geometry around the

metal ion center and the catenation ability of sulfur for I-IV-VI ternary chalcogenides, many kinds of Cu–Sn–E(S, Se) have been synthesized [4]. The ternary semiconductors Cu_2SnX_3 (X = S, Se) are found frequently as secondary phases in synthesized Cu_2ZnSnS_4 and $Cu_2ZnSnSe_4$ samples ,as candidates for low-cost thin-film solar-cell absorbers, quaternary semiconductors Cu_2ZnSnS_4 (CZTS) and $Cu_2ZnSnSe_4$ (CZTSe) have been studied intensively in the past five years [5].The research groups have been focusing their attention to this compound to increase the efficiency in the near future, despite the advantages that come from CZTS, it shows a complex structure and requires very controlled growth conditions, If this process starts with metallic precursors, intermediate binary and ternary sulfides are formed, these compounds will remain after the end of the growth process if the composition and the sulfurization conditions are carefully controlled, among these ternary sulfides, Cu_2SnS_3 is the most relevant compound[6]. The ternary Cu–Sn–S (CTS) system belongs to group I–IV–VI semiconductors which have attracted great attention because it's a potential earth abundant absorber material for photovoltaic devices application, light emitting diode, nonlinear optical materials, photo catalytic activity and lithium-ion electrode materials due to suitable optoelectronic properties and attractive raw-material features depending on its crystal structure, and their outstanding optical–thermal–mechanical properties [2,7,8]. CTS consists of low-cost non-toxic and abundant elements [8], and it is a p-type[9], with narrow direct band-gap semiconductor [10,11] ranging from 0.87–1.77 eV and exhibits high optical absorption coefficient ($>10^4$ cm^{-1}) [12]. Therefore Cu_2SnS_3 used in the heart of a thin films solar cell as the absorber layer which efficiently harvests sunlight [13].

Cu_2SnS_3 exists in a number of polymorphs, One of them, the cubic Cu_2SnS_3, is a high temperature polymorph ($>775\ ^{\circ}C$) and is not likely to appear in kesterite thin films due to the fact that typical growth temperatures are limited to $600\ ^{\circ}C$ [3].

This paper reports the impact of thickness and annealing temperatures on the structural, morphological, and optical properties of CTS thin films which deposited by flash thermal evaporation technique.

Experimental procedure

CTS alloy has been prepared with appropriate weight percentage (2:1:3) using high purity elemental Cu (Carloerba), Sn (England), and S (Ferac Berlin) which about 99.999 %. The elemental analysis of this alloy was carried out by using energy-dispersive X-ray spectroscopy (EDS) detector (Bruker nano GmbH, Germany) coupled with SEM model (Inspect S50 system) which give morphology of this alloy, also X-ray powder diffraction (XRD) investigated by (Miniflex II Rigaku company, Japan). X-ray diffractometer using Cu K_α radiation ($\lambda=1.5418$ A°). Cu_2SnS_3 alloy used as a source material to prepare thin films which deposited by flash thermal evaporation technique with different thickness with rate of deposition equal to 3.808 nm/min at high vacuum (10^{-5} mbar) using Edward Auto 360 vacuum coating unit.

The annealing process was carried out to prepare films in vacuum at 473 K for 1h. The structures of as deposited and annealed films were investigated. Also, topography of the films surface were studied by employing atomic force microscope (AFM) (AA3000 Scanning probe Microscope SPM, tip NSC35/AIBS from Angstrom Advanced Inc., USA). UV-visible absorption spectra were obtained using a Shimadzu (UV-1650 PC) spectrophotometer over the wavelength range (300-1100) nm and calculated the optical properties of as

deposited and annealed films with different thicknesses (500, 750, and 1000) nm.

Results and discussion
1. Composition analysis by EDS technique

Energy Dispersive X-ray Spectroscopy (EDS) technique was used to determine the amount or concentration of the elements (Cu, Sn, S) in the alloy depending on the standard of these elements. Fig.1 shows

EDS spectrum of CTS alloy. From this figure the peaks of Cu, Sn, and S elements can be recognized, this means that the alloy quality is good since there is no presence of other elements observed. Table 1 illustrates that the real phase of the sample equal to 60% and the secondary phase equal to 40%, and the S ratio equal to 2.09, this ratio doesn't reach to the essential value of the compound that equal to 3, So CTS is rich with Sn and poor with Cu and S.
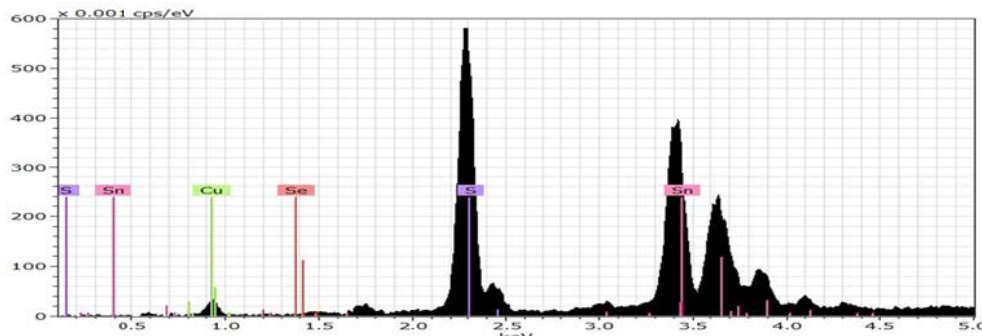

Fig. 1: EDS chart of CTS compound.

Table 1: Elemental compositions and ratios of real and secondary phases of CTS compound from EDS data.

Sample	Wt ratio % of EDS			Percentage Ratio % of EDS			Formula Exp. of moles	Real phase of formed film%	Secondary phase%
	Cu	Sn	S	Cu	Sn	S			
Cu_2SnS_3	20.35	45.73	35.36	20.06	45.07	34.85	$Cu_{1.2}Sn_{2.7}S_{2.09}$	60	40

2. Structure measurements
2.1 Scanning electron microscopy (SEM)

The surface morphology results of prepared CTS alloy was studied by SEM images with two magnification value as

shown in Fig. 2. This figure show that the surface with black background, compressed and nubby grains. Also there are some white grains that may be belong to Sn existence, this result agrees with Zhao and Cheng [9].
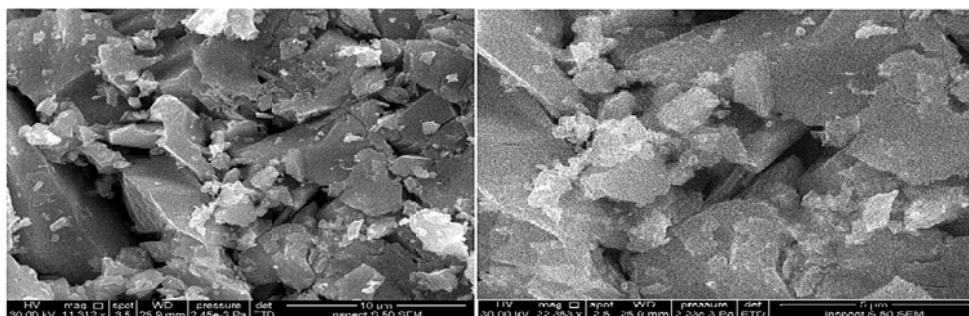

Fig.2: Two magnification of SEM images for bulk CTS.

2.2 X-ray diffraction measurements

XRD using to investigate the structure of semiconductor material and to observe the structure changes after evaporation. The effect of films thickness (500,750 and 1000) nm, and the heat treatment (473 K) on the films structure has been studied. X-ray diffraction pattern of bulk CTS showed that the sample has a polycrystalline structure as shown in Fig.3. The results of bulk CTS reveals that the cubic phase appears with preferred orientation along (111) direction at 2θ around 28.326° dominates, the data compared with JCPDS Card number 01-089-2877, this result is agreement with Liang et al. [3] and Fernandes et al.[5].

The structural parameters like inter planer spacing, miller indices, and crystallite size for CTS alloy are shown in Table 2.
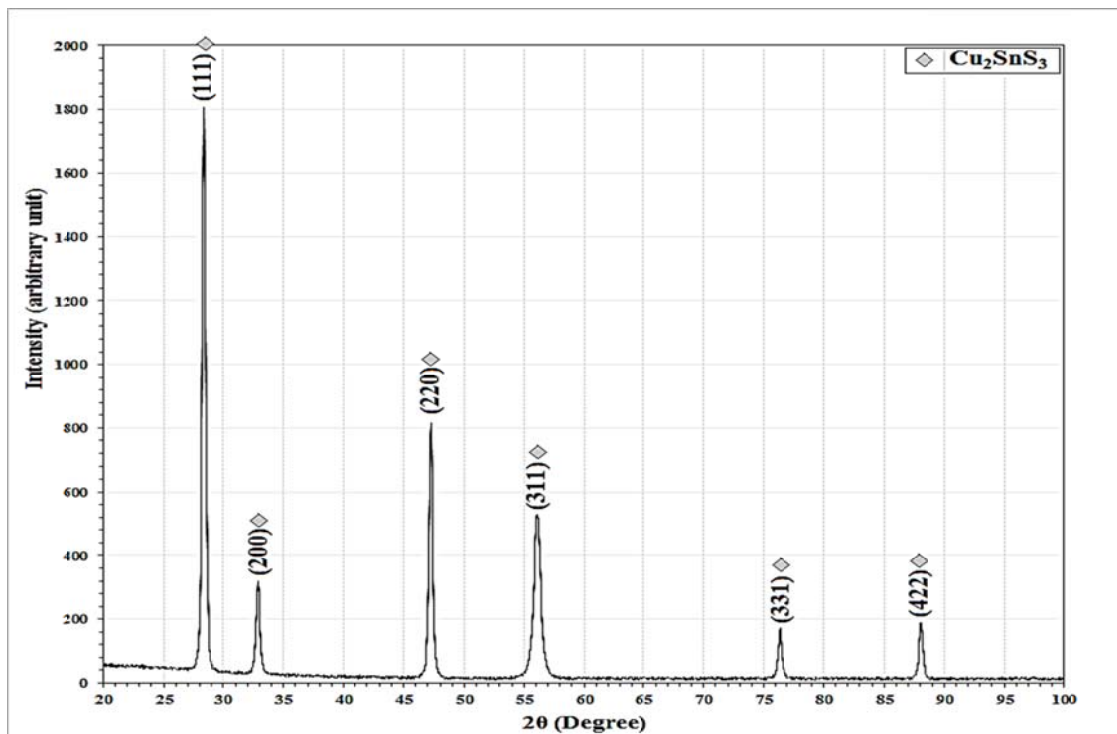

Fig. 3: X-ray diffraction pattern for CTS powder.

Table 2: Structural parameters viz. inter-planer spacing, miller indices, and crystallite size of bulk CTS.

Sample	2θ (Deg.)	d_{hkl} Exp. (Å)	d_{hkl} Std .(Å)	hkl	FWHM (Deg.)	Crys.Size (nm)	Phase
Cu_2SnS_3	28.3267	3.1481	3.13509	(111)	0.3060	26.8	Cubic-Cu_2SnS_3
	32.8738	2.7223	2.71507	(200)	0.3530	23.5	Cubic-Cu_2SnS_3
	47.2520	1.9221	1.91984	(220)	0.3290	26.4	Cubic-Cu_2SnS_3
	56.1140	1.6377	1.63725	(311)	0.6350	14.2	Cubic-Cu_2SnS_3
	76.3567	1.2462	1.24576	(331)	0.3530	28.6	Cubic-Cu_2SnS_3
	88.0380	1.1085	1.10842	(422)	0.3530	31.3	Cubic-Cu_2SnS_3

The X-ray diffraction pattern of as deposited and annealed Cu_2SnS_3 films for different thickness (500,750 and 1000) nm are shown in Fig. 4 and Table 3.
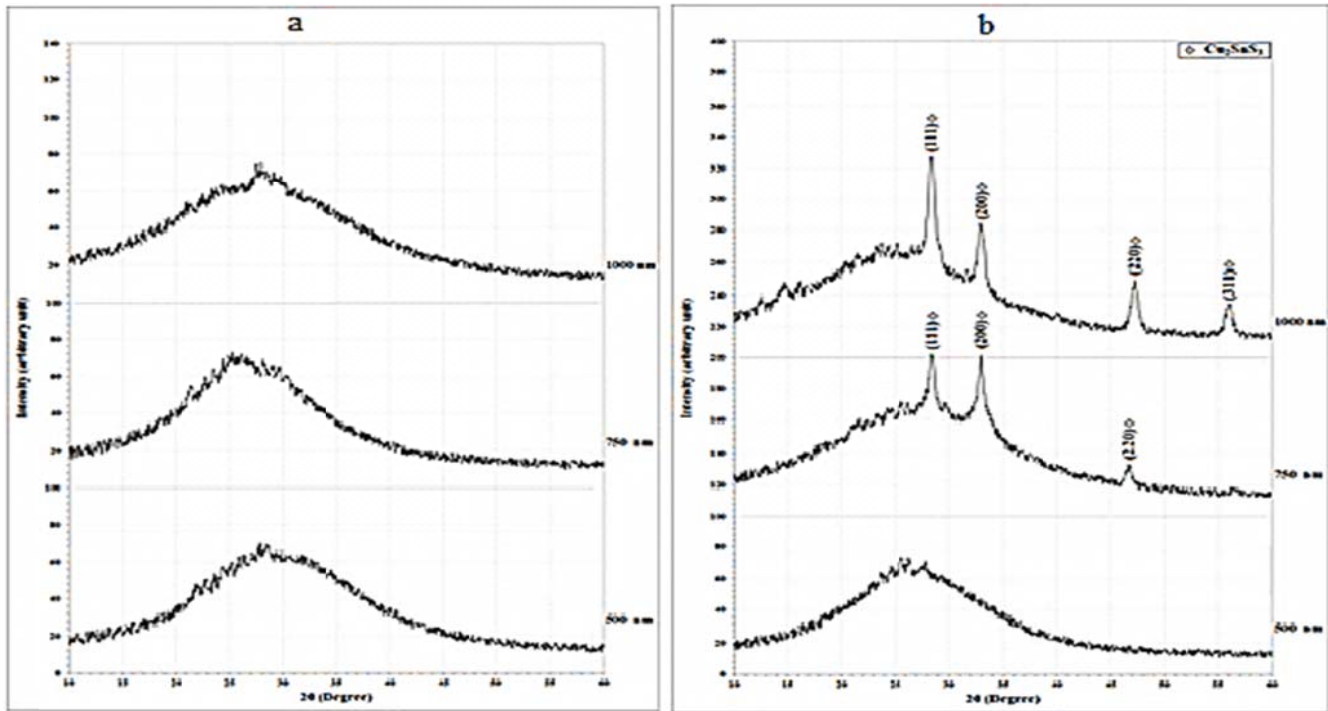
123

Fig. 4: X-ray diffraction pattern for CTS films at different thickness a-as deposited b-annealed at 473 K.

As deposited CTS films for different thickness show an amorphous structure. Annealed CTS films with thickness 500 nm also show an amorphous structure, while the annealed film with thickness 750 nm have three peaks with good intensity corresponding to (111), (200), and (220) for cubic structure around 2Θ equal to 28.460°, 32.976°, and 46.701° respectively. The annealed films with thickness 1000 nm have four peaks appeared with high intensity corresponding to (111), (200), (220), and (311) around 2Θ equal to 28.420°, 32.972°, 47.232°, and 56.013° respectively. However there is no binary phase formed, this means the compositions are good, and there is no re-evaporation of S from the growing films. Generally, CTS thin films were amorphous and become polycrystalline by annealing and have a good peaks than as deposited films because annealing enhanced the properties of films, the peak intensity increased when thickness increased because of thickness make the matter of films more compact then reduce the defect in the these films.

Table 3: Structural parameters viz. inter-planar spacing, miller indices, and crystallite size of CTS films annealed at 473 K with different thicknesses.

t (nm)	2θ (Deg.)	d_{hkl} Exp. (Å)	d_{hkl} Std. (Å)	hkl	FWHM (Deg.)	Crys.Size (nm)	Phase
500	-	-	-	-	-	-	Amorphous
750	28.4600	3.1337	3.13509	(111)	0.6350	12.9	Cubic-Cu_2SnS_3
	32.9760	2.7141	2.71507	(200)	0.3760	22.0	Cubic-Cu_2SnS_3
	46.7012	1.9435	1.91984	(220)	0.5140	16.8	Cubic-Cu_2SnS_3
1000	28.4200	3.1380	3.13509	(111)	0.7290	11.2	Cubic-Cu_2SnS_3
	32.9720	2.7144	2.71507	(200)	0.7240	11.4	Cubic-Cu_2SnS_3
	47.2320	1.9228	1.91984	(220)	0.7210	12.0	Cubic-Cu_2SnS_3
	56.0130	1.6404	1.63725	(311)	0.7340	12.3	Cubic-Cu_2SnS_3

2.3 Atomic Force Microscopy (AFM)

AFM is a useful technique for determining surface topography and regarded the most effective ways due to its high resolution and powerful analysis. The three dimensional AFM images and histogram of as deposited and annealed CTS thin films prepared by flash thermal evaporation with thickness equal to 1000 nm are shown in Fig. 5 and Table 4. These images revealed that the film is covered by uniform, homogeneous and tightly adherent, nano crystallites, having spherical grains without any voids or cracks.

Also these images show that the CTS thin films have continuous grnular mrphology. The spherical grains for CTS was reported by Tiwari et al. [12], who they prepared the CTS films by direct liquid coating.

The grain size for as deposited CTS films increases from 87.78 nm to 102.02 nm when film annealed at 473 K .This behavior occur due to structure improvement. while the root mean square roughness (RMS) decrease as summarized in Table 4, this means the average roughness decrease with annealing temperature.
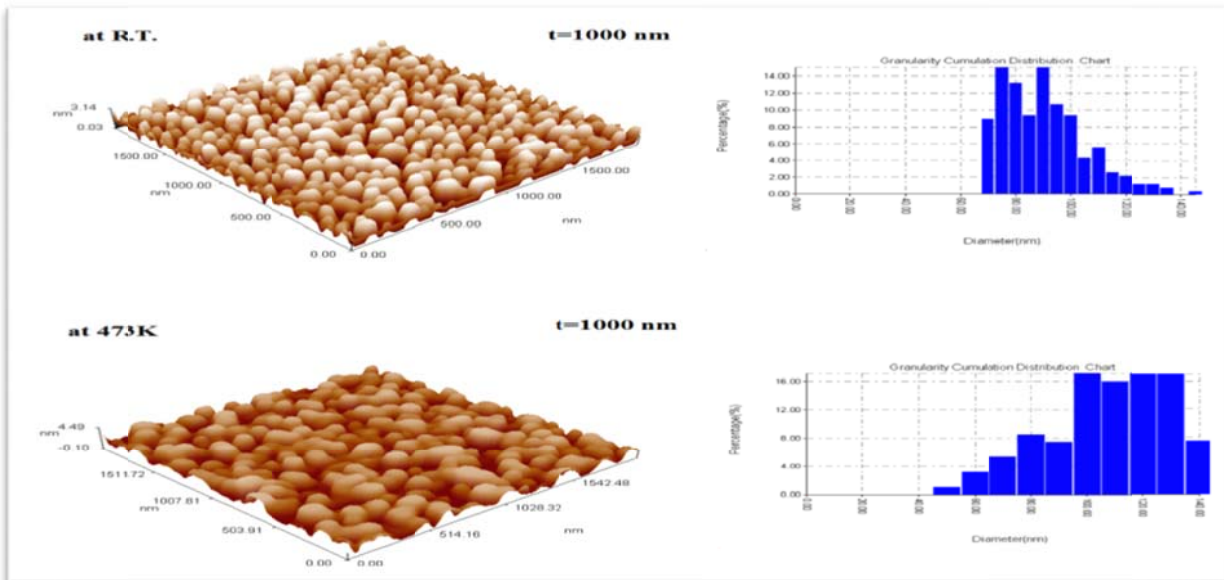

Fig. 5: AFM topography image of thin CTS films with t= 1000 nm that prapared at R.T. and annealed at 473 K.

Table 4: Average grain size, average roughness, and root mean square for CTS.

Thickness (nm)	Temp. (K)	Grain Size (nm)	Average Roughness(nm)	Root Mean Square (nm)
1000	R.T.	87.78	0.777	0.897
	473	102.02	0.712	0.819

3. Optical measurements

The optical transmittance spectra of CTS thin films deposited at room temperature on glass substrates with different thicknesses (500, 750 and 1000) nm and annealed at 473 K, are shown in Fig. 6. From this figure, we can observed there is no interference fringes, this occurs

due to the optical scattering phenomena in such film.

The transmittance of all deposited thin films increases with increasing of wavelength (λ), and decrease with increasing films thickness from 500 nm to 1000 nm, this occurs because increasing film thickness lead to decrease the defects

and voids which result to increase the films absorption, as a result the transmittance decrease. The shift of transmittance toward higher wavelength with increasing thickness explains the shifting of the absorption edge towards lower energies.
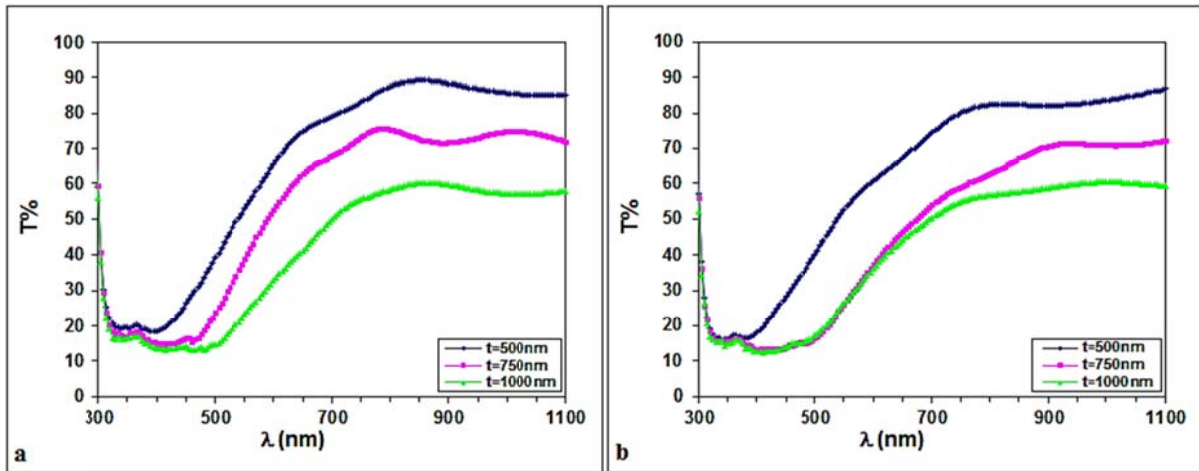

Fig. 6: The transmittance versus the wavelength for CTS films at different thickness a-as deposited b-annealed at 473 K.

From Table 5 we can observe that the optical absorption coefficients for all films were fairly high values reached above 10^4 cm^{-1}, which means that there is a large probability of allowed direct transitions. The absorption coefficient dependence on the film thickness as a function of wave length for CTS films, it was notice from Table 5 that α increase with increasing films thickness for as deposited and annealed films.

In order to verify the nature of the band gap of Cu_2SnS_3, we plot $(\alpha h\upsilon)^2$ as a function of photon energy ($h\upsilon$) for as deposited and annealed films with different thickness (500, 750, 1000) nm as shown in Fig. 7 a and b respectively.

The linear dependence in the high-energy range of the spectra observed in this plot indicated that Cu_2SnS_3 has a direct band gap. The optical energy gap decreases with increasing films thickness as cleared from Fig. 7 and Table 5.
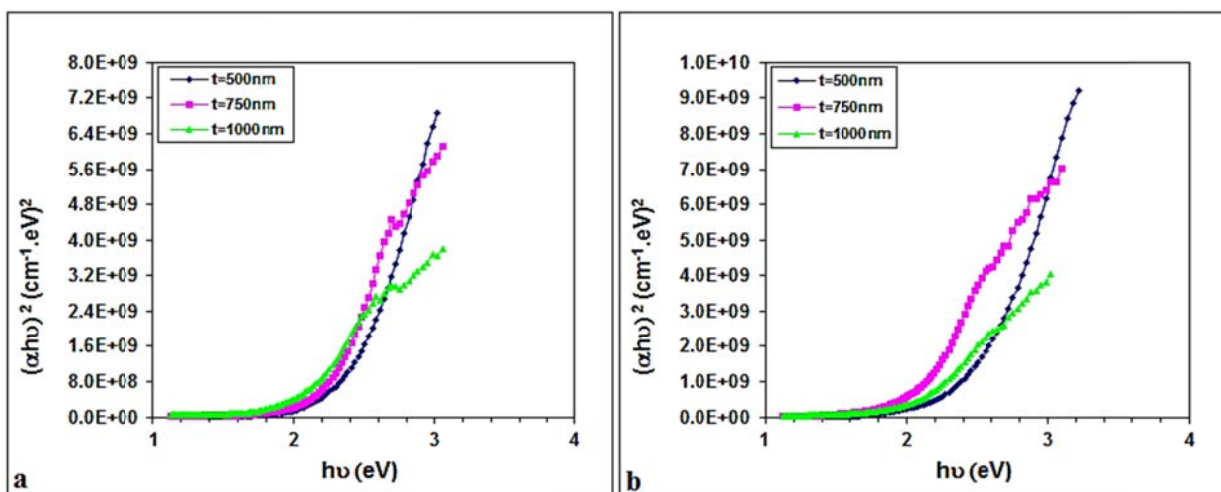

Fig. 7: The variation of $(\alpha h\upsilon)^2$ versus the photon energy ($h\upsilon$) for CTS films at different thickness a-as deposited b-annealed at 473 K.

It is obvious that the optical energy gap (E_g) decrease from 2.41 eV to 1.92 eV for 500 nm, and 1000 nm respectively, the last result is approach to Zhao and Cheng results [9]. This decrement of E_g with increasing thickness may be related to increase the absorption coefficient. E_g decreasing by increase thickness because it is well known that E_g value of bulk material is lower than that of film sample, that means there is a reduction occur in E_g values, since the structure will be approach from that of bulk material. Generally, E_g influence by annealing temperature where it increases when films annealed.

In general, the the extinction coefficient (k) increase for as deposited and annealed films at 473 K with thickness increasing due to increase of the grain size.

For as deposited CTS films, the refractive index (n) increased from 2.34 to 2.52 when thickness increased from 500 nm to 1000 nm. n increased by annealing films at 473 K.

It is obvios from Table 5 that the behavior of the real part of dielectric constant (ε_r) and imaginary part (ε_i) have the same as that of n and k respectively with the variation of thickness.

It can be observed that the real dielectric constant (ε_r) for as deposited CTS films increased from 5.48 to 6.39 by increasing thickness from 500 nm to 1000 nm, while imaginary dielectric constant part (ε_i) increased from 0.158 to 0.26 for CTS films. Generally, ε_r and ε_i increase by increasing thickness.

Table 5: The values of E_g^{opt} and optical constants at λ=600 nm for as deposited and annealed CTS films with different thickness.

Alloys	Thickness (nm)	Temp.(K)	$E_g^{opt.}$ (e V)	$\alpha *10^4$ (cm^{-1})	n	k	ε_r	ε_i
	500	R.T.	2.41	0.707	2.34255	0.03148	5.48641	0.15806
		473	2.52	0.83	2.44435	0.03962	5.973304	0.19372
	750	R.T.	2.22	0.853	2.578654	0.04071	6.64779	0.20995
Cu$_2$SnS$_3$		473	2.05	1.31	2.6085	0.06255	6.800408	0.32633
	1000	R.T.	1.92	1.11	2.528997	0.05322	6.39299	0.26919
		473	1.97	1.01	2.59411	0.04841	6.72707	0.2512

Conclusions

Effect of film thickness and annealing temperature on the structural, morphological, and optical properties of Cu$_2$SnS$_3$ films deposited by flash thermal evaporation technique were investigated. X-ray diffraction study of the CTS powder shows that this material crystallizes in cubic structure. The structures of as deposited films have amorphous structure and improve with annealing. AFM measurement showed that the average grain size increase with annealing. The results of the optical characterization revealed that the CTS films of thickness 1000 nm have low transmittance in the visible range. The results also revealed that the Cu$_2$SnS$_3$ films have direct band gap of about 1.92 eV. This indicates that these films are active in the visible portion of the spectrum and could be employed as absorber layer in the solar cells.

References

[1] Q. Chen and Di Ma, Hindawi Publishing Corporation International Journal of Photoenergy, 2013 (2013) Article ID 593420, 1-5.
[2] M. Adelifard, M. Mohagheghi, H. Eshghi, Phys. Scr., 85 (2012) 1-4.
[3] X. Liang, Q. Cai W. Xiang, Z. Chen, J. Zhong, Y. Wang, M. Shao, Z. Li, J. Mater. Sci. Technol., 29, 3 (2013) 231-236.
[4] Y. Zhai, S. Chen, J.Yang, H. Xiang, X. Gong, A. Kang, S. Wei, Physical Review, 84 (2011) 075213.

[5] P. Fernandes, P. Salomé, A. da Cunha, Physical Review, 84, 7 (2011) 1-6.

[6] J. Han, Y. Zhou, Y.Tian, Z. Huang, X. Wang, J. Zhong, Z. Xia, B. Yang, H. Song, J. Tang, front. Optoelectrron, Springer – Verlage Berline Heidelberg, (2014).

[7] T. Nomura, T. Maeda, T. Wada, 5. Japanese Journal of Applied Physics, 53 (2014) 1-6.

[8] M. Berg, R. Djemour, L. Gütay, G. 6. Zoppi, S. Siebentritt, P. Dominik, Thin Solid Films, 520 (2012) 6291–6294.

[9] P. Zhao and S. Cheng, Hindawi Publishing Corporation Advances in Materials Science and Engineering, 2013 (2013), Article ID 726080, 1-4.

[10] V. L. Shaposhnikova, A. V. Krivosheevaa, V. E. Borisenkoa, J.-L. Lazzarib, Science Jet, 520, 19 (2012) 1-15

[11] N.Aihara, A. Kanai, K. Kimura, M. Yamada, K. Toyonaga, A. Takeuchi, H. Katagiri, Japanese Journal of Applied Physics, 53 (2014) 012301.

[12] Devendra Tiwari, T. K. Chaudhuri, T. Shripathi, and U. Deshp, AIP Conf., 1447 (2012) 1039-1040.

[13] M.Dominik Berg, R. Djemour, L. Gutay, S. Siebentritt, P. Dale, X.Fontane, V. Izquierdo-Roca, A. Pe´rez-Rodriguez, Applied Physics Letter, 100 (2012) 192103.